

abstract

Bubble chamber is a device we use to study the behaviors of very small particles. In this experiment we were to study the activities of K^- meson by scanning the photographs of 70 mm film of real ~~experiment~~^{done with} bubble chambers, with K^- beam of momentum 1.5 GeV/c entering the chamber filled with liquid hydrogen of density approximately 0.06 gm/cm^3 , operating at the Berkeley Bevatron in the 1960's. We obtained

$$\tau = (1.04 \pm 0.05) \times 10^{-8} \text{ sec},$$

$$\sigma_{el} = (0.82 \pm 0.04) \times 10^{-30} \text{ m}^2,$$

and

$$\sigma_{tot} = (3.51 \pm 0.16) \times 10^{-30} \text{ m}^2.$$

We also approximated the proton's effective radius to be

$$R_p = (5.89 \pm 0.14) \times 10^{-16} \text{ m}$$

For K^- decays we obtained the branching ratio of the "tau" (τ) mode, $K^- \rightarrow \pi^+ \pi^- \pi^-$,

$$BR = (5.56 \pm 0.10)\%.$$

Introduction

Decays and interactions are governed by many conservation laws. These include the conservation laws of (angular) momentum, electric charge, baryon number, and lepton number for all kinds of decays and interactions. For strong interactions, isospin, parity, and flavor are also conserved. K^- mesons incident on hydrogen nuclei (protons) with momentum 1.5 GeV/c produce many final states, including both long-lived ($>10^{-10}$ sec) particles and short-lived

"resonances." In this laboratory we will concentrate on the long-lived final states, which can be identified by scanning rather than quantitative momentum measurement of the tracks. Selection rules that require weak decays of strange final states cause long strange particle lifetimes. This experiment introduces us to the realm of elementary particles and the conservation laws that govern their interactions and decays.

Theory

When K^- enters the region of hydrogen, the number of K^- decreases due to decays and the inelastic interactions between K^- and the hydrogen nuclei.

If we have a large collection of K^- , N_0 , at time t , then $N\Gamma dt$ of them would decay in the next instant dt , where Γ is the decay rate-- the probability per unit time that any given K^- will disintegrate. The mean lifetime is simply the reciprocal of the decay rate: $\tau = \frac{1}{\Gamma}$. For relativistic K^- traveling in the medium of hydrogen

$$dt = \frac{dx}{v} \quad \text{not } v, \nu \text{ usually means neutrino in particle physics.}$$

therefore

$$dN = -\Gamma N dt = -\frac{N dx}{v \tau}$$

It follows that

$$N_t = N_0 \exp\left(-\frac{x}{v \beta c \tau}\right) \quad (1)$$

The K^- number N decreases in the hydrogen medium at a rate dN/dt , with respect to the

K^- path length, is directly proportional to the number of incident K^- beam N , the cross section σ of all the inelastic interactions, and the number of hydrogen nuclei per unit volume N_H . The number of proton in unit volume is simply given by

$$N_H = \frac{N_a \rho}{A}$$

where N_a is the Avogadro's number, ρ is the mass density of proton in liquid hydrogen, and A is the atomic number of proton. Therefore

$$\frac{dN}{dx} = -\frac{\sigma N_a \rho N}{A}$$

It follows

$$N = N_0 \exp\left(-\frac{x N_a \sigma \rho}{A}\right) \quad (2)$$

Combining Eqn (1) and (2), we obtain the equation for the number of K^- as a function of path length x in the hydrogen medium due to both decays and all the inelastic interactions

$$N = N_0 \exp\left(-\frac{x}{\gamma \beta c \tau}\right) \exp\left(-\frac{x N_a \sigma \rho}{A}\right) \quad (3)$$

For short average K^- path length within the fiducial volume, Δx , we approximate

$$\frac{\Delta N_D}{\Delta x} = \frac{dN_D}{dx} \quad \text{and} \quad \frac{\Delta N_I}{\Delta x} = \frac{dN_I}{dx}$$

where ΔN_D and ΔN_I are the numbers of all decays and inelastic interactions, respectively.

Since decay in flight affects the number of K^- , it affects the number of possible inelastic interactions, and vice versa. We have to modify the number of K^- to

$$N = N_0 - \frac{\Delta N_I + \Delta N_D}{2}$$

according to Appendix (1). Therefore we obtain

$$\frac{\Delta N_D}{\Delta x} = \frac{1}{\gamma \beta c \tau} \left(N_0 - \frac{\Delta N_I + \Delta N_D}{2} \right) \quad (4)$$

and

$$\frac{\Delta N_I}{\Delta x} = \frac{N_a \rho \sigma}{A} \left(N_0 - \frac{\Delta N_I + \Delta N_D}{2} \right) \quad (5)$$

Apparatus and Procedure

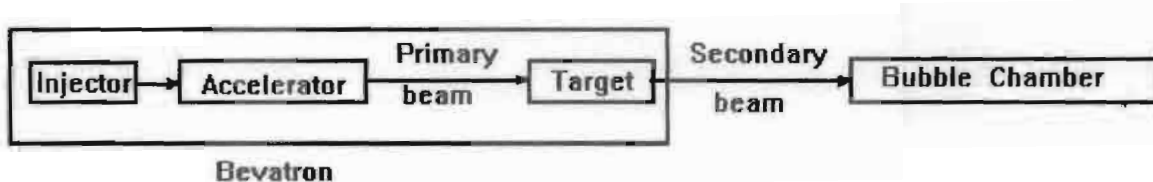


Figure 1: Experimental set-up for the production of K^- and bubble chamber analysis.

The K^- 's are produced in the Bevatron, a large and complex device. Positively charged protons are injected into the Bevatron with an energy typically low. The protons are accelerated in a circular track with magnetic field perpendicularly across it until they reach the desired energy. Then the accelerating voltage is turned off so that the proton gradually spiral inward and strike the target. (See Fig. 2)

At this point an array of particles of many kinds at a spectrum of energies are produced. This is the secondary beam. Using a bending magnet to select the desired moment and a velocity spectrometer to select the desire type of particle, we obtain the desired K^- beam, which is then lead to the bubble chamber for study.

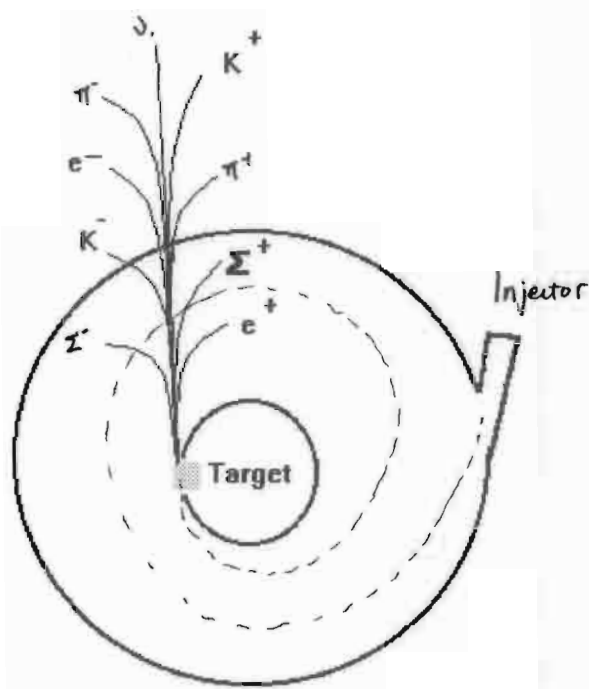


Figure 2: Accelerator and target for production of K^- .

The bubble chamber consists of a closed vessel containing a liquid at a temperature slightly above its normal boiling point but under a sufficient pressure to prevent it from boiling. The pressure of the liquid is suddenly released, and for a fraction of a second, the liquid hydrogen does not boil but in a superheated state. If during this brief period of time, a charged particle (K^- or other charged particles due to decays or inelastic interactions) passes through the liquid, it will serve as a nucleon for the superheated hydrogen nuclei to form bubbles. Therefore a track is left indicating the path of the charged particle. The neutral particles cannot [why not?] serve as a nucleon and therefore leave no visible tracks. Pictures are taken from three different angles at this moment to record the event. The bubble then collapses under recompression, and the cycle is repeated. A known magnetic field is imposed perpendicularly across the chamber so that from the direction a charged particle curves we can distinguish its sign of charge and from the curvature we can calculate its momentum.

The above procedures to produce the films were actually done at the Berkeley Bevatron in the 1960's. Our procedure in this laboratory is to scan and study 500 of these films. We selected a fixed fiducial region and concentrated on the events taking place in the region, ignoring all the events outside of it. We recorded all events found in the fiducial region with frame number, rough location within the chamber, and the event type. For every tenth frame, we recorded the number of good beam tracks that enter the fiducial region to obtain the total number of incoming tracks.

Data

Roll number: 5450

Frame Number	No Event	Number of Tracks	Collision	Interaction	Decay	Tau" Decay	Location	Length
394	No							
395	No							
396				4-P			0.8/290	8.9
397	No							
398	No							
400	No							
401					1-P		0.5/240	11.5
402				2-P			0.6/180	21.3
403	No							
404		13			1-P		0.5/120	25.0
405					1-P		0.6/120	22.5
406	No							
407	No							
408					1-P		0.5/270	6.8
****					1-P		0.3/180	18.5
409				0-P			0.7/140	28.4
410					1-P		0.2/100	23.3
411				4-P			0.5/240	12.3
412	No							
413	No							
414		10			1-P		0.8/270	1.0
415			2-P				0.4/170	19.5
416	No							
417	No							
418					1-P		0.7/250	2.7
419					1-P		0.8/230	4.5
****					1-P		0.7/230	6.1
420	No							
421	No							
422	No							
423					1-P		0.3/180	19.7
424		5	2-P				0.7/140	26.9

426	No						
427				0-P + V			0.5/230 7.2
****			2-P				0.4/180 16.1
428	No						
429				2-P			0.6/120 25.3
****					1-P		0.5/190 14.2
430				4-P			0.3/110 23.6
431	No						
432			2-P				0.3/180 17.8
433					1-P		0.3/210 14.5
****			2-P				0.3/130 22.3
434					1-P		0.4/150 21.4
****				0-P			0.6/140 22.9
****			2-P				0.7/130 26.2
435	No	8					
436			2-P				0.2/260 13.2
****				2-P			0.4/120 26.0
437	No						
438				2-P			0.5/130 24.0
****					1-P		0.6/140 23.4
439					1-P		0.5/170 21.4
440	No						
441	No						
442					1-P		0.3/190 17.4
443				4-P			0.4/250 10.6
444				2-P			0.8/260 3.9
****					1-P		0.9/90 28.1
445		11		2-P + V			1.0/270 0.4
446					1-P		0.9/280 2.1
447				0-P			0.3/280 10.9
448				0-P			0.4/220 12.8
449	No						
450				2-P			0.2/230 13.4
451					1-P		0.5/280 7.2
452				2-P + V			0.6/230 5.1
453	No						
454					1-P		0.5/100 29.3
455		11			1-P		0.7/240 3.0
****				2-P			0.7/230 8.2
456	No						
457				2-P			0.3/180 19.2
458	No						
459				2-P			0.8/270 0.3
460	No						
461					1-P		0.2/100 23.6
462				2-P			0.7/180 17.0
463	No						
464	No						
465	No	10					
466	No						
467	No						
468					1-P		0.7/230 7.8
469	No						
470					1-P		0.4/230 12.4
471	No						
472					1-P		0.9/240 1.9
473				0-P			0.7/270 10.8
474	No						
475	No	10					
476	No						
477	No						
478				2-P			0.8/260 1.0
479	No						
480				0-P			0.8/220 8.0
****				2-P			0.3/180 16.1
481					1-P		0.5/230 12.9

482					1-P		0.7/190	14.6
483					2-P		0.4/260	9.3
484	No							
485	No	12						
486	No							
487				0-P + V			0.9/240	4.2
488	No					3-P	0.8/140	27.1
489								
490	No							
491	No							
492	No							
493	No							
494				0-P			0.3/260	11.2
****					1-P		0.4/200	17.5
495	No	5						
496					1-P		0.6/250	5.3
497				0-P			0.7/280	2.6
498	No							
499	No							
500	No							
501	No							
502				0-P			0.8/240	4.4
5.3				2-P			0.4/130	26.2
504	No							
505	No	6						
506	No							
507					1-P		0.7/200	14.7
***				2-P + V			0.7/40	26.6
508				4-P			0.7/270	1.1
****					1-P		0.8/240	4.9
509	No							
510				2-P			0.5/170	18.8
511			2-P				0.4/130	24.4
****				2-P			0.4/140	23.0
512						3-P	0.1/20	18.0
513	No							
514	No							
515	No	6						
516	No							
517				2-P + V			0.8/240	1.9
518								
519			2-P				0.6/260	4.6
520	No							
521						3-P	0.5/240	8.3
522	No							
523	No							
524				0-P			0.4/110	24.5
525		11		4-P			0.5/130	27.2
526	No							
527					1-P		0.4/270	8.4
528				2-P			0.8/260	0.5
529	No							
530					1-P		0.6/230	9.5
****				2-P + V			0.5/190	16.3
531	No							
532				2-P + V			0.5/230	8.6
****					1-P		0.7/100	28.3
533	No							
534				2-P			0.4/190	16.1
535	No	6						
536					1-P		0.2/140	19.4
537					1-P		0.8/270	0.5
538				2-P + V			0.7/190	13.5
539	No							
540	No							
541					1-P		0.6/210	11.5

542	No						
543				2-P		0.6/230	10.4
****				2-P		0.8/250	0.4
544					1-P	0.1/190	19.2
545		12			1-P	0.9/240	3.3
546	No						
547	No						
548	No						
549	No						
550			2-P			0.4/180	18.2
551				2-P		0.9/240	2.6
552	No						
553	No						
554	No						
555	No	4					
556	No						
557					1-P	0.9/140	27.3
****			2-P			0.8/140	27.5
558	No						
559					1-P	0.5/120	25.1
****				2-P		0.6/150	25.7
560	No						
561	No						
562				2-P		0.8/250	2.2
563	No						
564	No						
565	No	12					
566	No						
567	No						
568	No						
569				0-P		0.4/180	17.1
570	No						
571			2-P			0.1/80	20.7
572			2-P			0.6/240	7.8
573			2-P			0.2/230	14.6
574	No						
575		13		2-P		0.6/280	3.3
576				0-P		0.5/160	15.8
577					1-P	0.6/130	28.1
****			2-P			0.5/170	17.8
****			2-P			0.8/240	5.6
578					1-P	0.2/270	12.0
579			2-P			0.5/190	14.5
580					1-P	0.8/250	5.2
****			2-P			0.5/220	13.7
581			2-P			0.7/260	3.6
582					1-P	0.9/240	1.1
583	No						
584	No						
585	No	3					
586				0-P		0.9/230	0.3
****					1-P	0.8/230	3.3
****					1-P	0.2/210	14.3
587	No						
588						0.7/240	6.2
589	No						
590	No						
591				2-P		0.8/260	1.6
592	No						
593			2-P			0.2/180	16.8
594					1-P	0.5/250	7.7
595	No	9				0.8/260	1.0
596					1-P	0.4/270	7.8
****			2-P			0.5/240	8.1
597			0-P			0.4/230	11.5
598			2-P				

599			0-P		0.5/130	23.9
600			2-P		0.4/130	14.4
****			2-P		0.6/260	5.4
601				1-P	0.6/220	10.3
602	No					
603	No					
604	No					
605		10		1-P	0.4/230	9.0
606			0-P		0.8/240	3.9
****			2-P		0.3/190	16.0
607			2-P		0.2/100	21.6
608	No					
609	No					
610			2-P		0.5/190	15.1
611	No					
612	No					
613	No					
614	No					
615	No	9				
616			2-P		0.8/240	3.9
617			2-P		0.5/240	7.4
618	No					
619	No					
620	No					
621			2-P		0.2/180	16.9
622				1-P	0.8/140	26.0
623			2-P		0.6/250	5.4
624	No					
625	No	9				
626	No					
627			2-P		0.7/300	1.7
628	No					
629	No					
630			2-P		0.2/140	18.1
631			2-P		0.8/160	22.8
632	No					
633	No					
634			2-P		0.6/240	6.9
635	No	8				
636	No					
637			4-P + V		0.7/260	3.8
638	No					
639	No					
640	No					
641	No					
642			2-P		0.4/100	25.1
642	No					
644	No					
645	No	11				
646				1-P	0.6/270	2.3
647	No					
648			2-P		0.5/130	24.0
649			2-P		0.5/160	20.6
650	No					
651	No					
652	No					
653	No					
654	No					
655	No	9				
656	No					
657	No					
658	No					
659	No					
660				1-P	0.5/120	26.3
661	No					
662	No					

663	No						
664	No						
665		6			1-P	0.4/180	18.0
666				2-P		0.3/90	23.4
667	No						
668			2-P			0.5/100	25.7
****					1-P	0.8/140	27.0
669					1-P	0.7/150	24.9
670			2-P			0.8/260	2.4
671			2-P			0.9/250	0.6
672	No						
673						0.4/150	19.9
****			2-P			0.6/100	29.0
674					1-P	0.6/240	6.0
****					1-P	0.1/90	21.7
675	No	12					
676			2-P			0.8/240	6.7
677					1-P	0.3/190	15.0
678					1-P	0.7/240	7.8
****			2-P			0.6/240	9.0
****			2-P			0.7/270	4.4
679	No						
680	No						
681			2-P			0.5/120	20.8
****			2-P			0.2/260	12.7
682			2-P			0.6/240	7.3
683				2-P + V		0.8/220	8.6
684	No						
685		10			1-P	0.9/250	2.7
686			2-P			0.3/260	10.7
687					1-P	0.3/110	23.8
688			2-P			0.7/240	6.8
****			2-P			0.5/180	16.8
689			2-P			0.2/170	18.8
690				2-P + V		0.4/210	13.7
691					1-P + V	0.1/170	18.1
****					1-P + V	0.8/250	4.4
****			2-P + V			0.6/230	8.7
692	No						
693	No						
694			2-P			Center	13.9
****			2-P			0.5/230	9.6
****					3-P	0.5/230	10.8
695		12		2-P		0.6/230	12.7
696	No						
697					1-P	0.4/250	8.4
****			2-P			0.5/130	29.9
****					1-P	0.7/230	9.9
698					1-P	0.7/270	2.5
699	No						
700	No						
701					1-P	0.4/250	10.9
702			2-P			0.3/250	9.4
703					1-P	0.3/120	21.4
****			2-P			0.4/120	24.1
704					1-P	0.4/260	7.7
****			2-P			0.8/120	28.8
705	No	11					
706				2-P		Center	17.1
707	No						
708					1-P	0.3/90	24.9
709					1-P	0.9/250	3.7
****			2-P			0.7/250	7.6
****					1-P	0.6/130	22.7
****			2-P			0.5/110	25.9
710						0.8/280	0.6

711	No						
712					1-P	0.6/110	28.5
713				2-P		0.8/270	0.2
714	No						
715	No	12					
716	No						
717			2-P			0.7/200	12.5
718	No						
719	No						
720	No						
721	No						
722				1-P		0.3/270	13.0
723	No						
724				1-P		0.7/300	4.1
****				1-P		0.6/270	4.8
725		14		2-P		0.4/320	10.1
726	No						
727	No						
728	No						
729	No						
730	No						
731				1-P		0.6/240	8.4
732	No						
733	No						
734	No						
735	No	7					
736	No						
737	No						
738	No						
739				2-P		0.4/320	10.6
740	No						
741	No						
742				2-P		0.9/240	1.1
743					1-P	0.5/240	8.5
744	No						
745	No	4					
746	No						
747	No						
748				1-P		0.8/270	0.9
749	No						
750	No						
751	No						
752	No						
753				1-P		0.8/250	3.2
754				1-P		0.7/300	3.0
755	No	12					
756	No						
757	No						
758				1-P		0.8/260	0.5
759	No						
760				1-P		0.3/250	10.9
761				1-P		0.2/170	18.9
762				1-P		0.5/270	6.2
763	No						
764	No						
765	No	7					
766				1-P		0.6/260	2.8
767	No						
768				1-P		0.4/150	22.7
****			2-P			0.7/230	5.0
769			2-P			0.4/180	17.2
770	No						
771			4-P			0.7/230	9.1
772	No						
773	No						
774				1-P		0.8/270	1.1

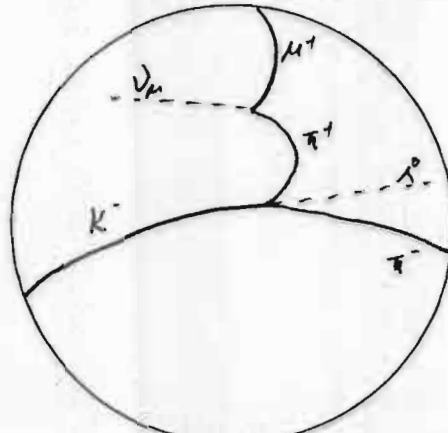
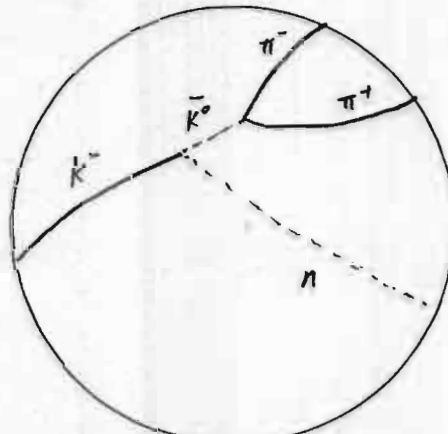
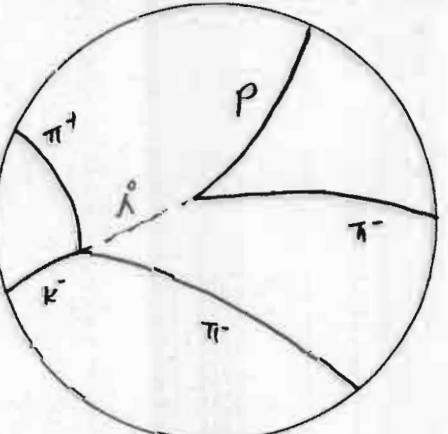
775	No	10						
776	No							
777	No							
778	No							
779	No							
780			2-P			0.2/110	21.6	
****			2-P			0.4/100	26.4	
781	No							
782			2-P			0.2/270	13.0	
783				1-P		0.5/230	10.1	
784			0-P			0.7/260	3.6	
****			2-P			0.5/290	6.2	
785	No	6						
786			2-P			0.1/180	17.5	
****			2-P			0.5/170	19.5	
787	No							
788	No							
789			2-P			0.5/90	26.9	
790				1-P		0.8/140	27.9	
791	No							
792			2-P			0.3/140	22.7	
793	No							
794	No							
795		15		2-P			0.3/190	15.9
796	No							
797			0-P			0.5/30	8.1	
798				1-P		0.6/220	11.6	
799	No							
800				1-P		0.6/170	20.6	
****				1-P		0.8/280	0.7	
801			0-P			0.2/170	19.5	
802	No							
803			2-P			0.6/210	11.9	
804	No							
805	No	14						
806			2-P			0.6/220	12.7	
807	No							
808				1-P		0.5/190	15.6	
****			2-P			0.5/260	7.4	
809	No							
810				1-P		0.6/170	19.0	
811	No							
812	No							
813	No							
814	No							
815		13	2-P			0.8/250	2.2	
816	No							
817			4-P			0.5/230	11.1	
****			2-P			0.4/90	24.8	
818			2-P			0.6/100	28.8	
819				1-P		0.3/240	11.8	
****			2-P + V			0.6/220	10.4	
820	No							
821				1-P		Center	16.9	
****			2-P			0.1/140	19.4	
822				1-P		0.6/140	22.5	
****				1-P		0.6/220	10.7	
823				1-P		0.5/220	12.7	
824	No							
825	No	12						
826	No							
827				1-P		0.7/180	17.8	
****				1-P		0.6/130	26.9	
828			2-P + V			0.8/260	1.5	
****			2-P			0.4/230	11.8	
829	No							

830	No						
831	No						
832			2-P + V			0.9/220	3.5
833			2-P			0.6/180	17.7
834	No						
835	No	10					
836			2-P			0.6/210	12.1
837				1-P		0.3/270	10.2
838	No				1-P		
839						0.5/190	14.9
840	No						
841	No						
842	No						
843	No						
844			2-P			Center	16.7
845		7					
846				1-P		0.8/260	1.6
847	No						
848	No						
849				1-P		0.5/240	7.7
850	No						
851	No						
852	No						
853			2-P			0.6/120	29.5
854	No						
855		10	2-P			0.3/100	24.1
856	No						
857				1-P		0.7/140	25.0
858	No						
859			2-P			0.3/150	21.6
****				1-P		0.8/270	1.3
****				1-P		0.5/300	0.1
****				1-P		0.4/300	8.4
860				1-P		0.9/230	3.3
****				1-P		0.7/140	25.8
****			2-P			0.6/260	6.0
861	No						
862			2-P			0.4/100	27.1
863					3-P	0.8/250	3.1
864			0-P			0.6/100	28.8
865		11		1-P		0.6/110	23.1
866				1-P		0.3/290	11.0
867	No						
868	No						
869	No						
870				1-P		0.2/230	14.1
871				1-P		0.8/250	4.4
872					3-P	0.8/170	20.5
873			2-P			0.4/140	23.5
874			2-P			0.8/270	1.1
****			2-P			0.7/140	25.2
875		14		1-P		0.7/230	6.7
876	No						
877	No						
878				1-P		0.3/240	10.6
879			4-P			0.4/140	24.1
880				1-P		0.2/170	20.7
881			0-P + V			0.8/280	2.8
882				1-P		0.2/180	17.4
883	No						
884			0-P + V			0.4/260	8.5
****			Z-P			0.7/220	9.9
****			2-P			0.8/170	21.2
885		10		1-P		0.1/120	19.4
886	No						
887			2-P			0.5/170	19.4

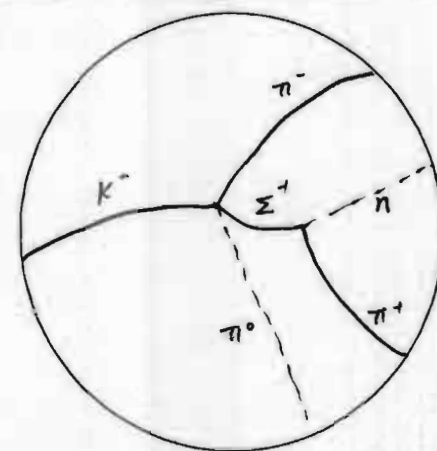
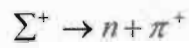
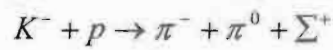
****				1-P		0.5/170	19.2
888			2-P			0.7/290	1.4
889	No						
890				1-P		0.9/250	0.3
****			2-P			0.4/60	27.6
891	No						
892				1-P		0.2/270	12.4
893				1-P		0.8/260	0.8
894				1-P		0.7/260	3.5
895		11		1-P		0.8/270	1.4
****			2-P			0.2/170	19.7
896			2-P			0.6/160	21.2
897	No						
898				1-P		0.4/180	17.6
899	No						
900			2-P			0.8/270	1.3
901				1-P		0.2/90	23.5
902				1-P		0.9/290	0.4
****				1-P		0.3/180	17.3
903	No						
904				0-P		0.6/270	3.5
****			2-P			0.5/270	6.3
905		9		1-P		0.3/180	16.4

Table 1: Measurement of events. Note that “n-P” indicates “n-prong,” “V” indicates “vee,” location is measured in polar coordinates with radii in unit of fiducial region radius and angle in unit of degrees, and path length is measured in centimeter. A “****” indicates a roll number identical to the roll number just above it.

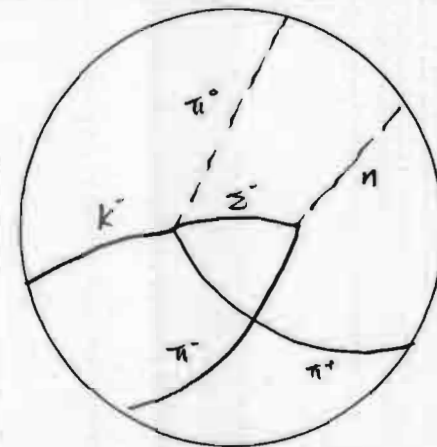
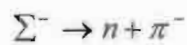
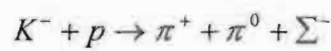
As we proceeded through the scan, we found roughly 20 different event. We recorded ten of them:

frame Number	Interactions	Observations
402	$K^- + p \rightarrow \pi^+ + \pi^- + \Lambda^0$ $\pi^+ \rightarrow \mu^+ + \nu_\mu$	
427	$K^- + p \rightarrow n + \bar{K}^0$ $\bar{K}^0 \rightarrow \pi^+ + \pi^-$	
445	$K^- + p \rightarrow \pi^+ + \pi^- + \Lambda^0$ $\Lambda^0 \rightarrow p + \pi^-$	

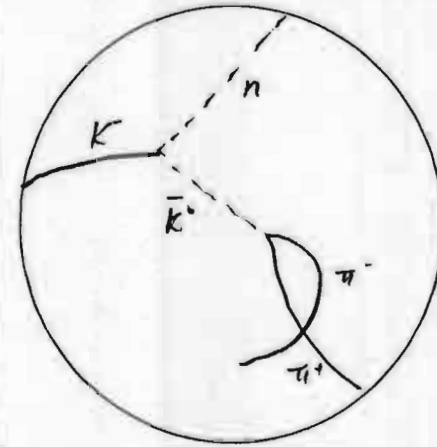
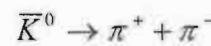
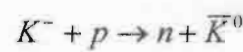
457



486



487



508	$K^- + p \rightarrow \pi^+ + \pi^- + \pi^- + \Sigma^+$ $\Sigma^+ + p \rightarrow \Sigma^+ + p$	
526	$\gamma \rightarrow e^+ + e^-$	
530	$K^- \rightarrow \mu^- + \nu_\mu$ $\mu^- \rightarrow e^- + \bar{\nu}_e + \nu_\mu$	

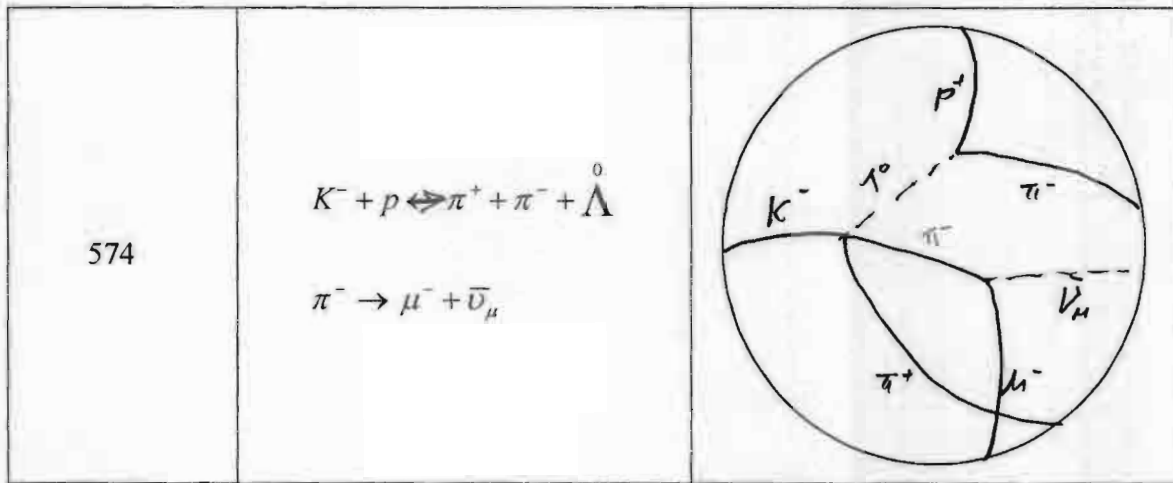


Table 2: Observation of events.

Analysis

Total number of decays (ΔN_D)	144
number of "tau" decays (N_τ)	8
Total number of interactions	137
Number of elastic collisions (ΔN_{el})	41
Number of inelastic interactions (ΔN_I)	178
Total number of tracks for the selected 50 films (N_{50})	486
Average track length for the 500 films before events (Δx)	0.2894m

Table 3: Summary of the events.

1) Branching ratio

From Table 3, we can easily find the branching ratio of "tau" decay for K^-

$$BR \equiv \frac{N_\tau}{\Delta N_D} = \frac{8}{144} = 5.56\%$$

Since N_t and ΔN_D are not statistically independent, the error for BR is propagated according to

$$\sqrt{\frac{8 \times 144}{(144 + 8)^3}} = 1.81\%$$

Therefore we obtained the branching ratio

$$\boxed{\text{BR} = (5.6 \pm 1.8)\%}$$

The value from the Particle Data Table in the library is $(5.59 \pm 0.05)\%$. Our experimental result falls in this range.

2) Total number of incident K^- particles for 500 films

From Table 3 the total incoming K^- particles for 50 random films is 486, and the standard deviation is given by Poisson statistics to be $\sqrt{486} = 22.0$. Therefore the total number of incident K^- particles for 500 films is simply given by

$$N_0 = (486 \pm 22.0) \times 10 = \boxed{4900 \pm 200}$$

3) Correction for the cross section area

The difficulty in observing and identifying a small angle of $K^- p$ elastic scattering introduces a systematic error to the observations. Assume the bubble size is about 0.3 mm and that for recoil lengths greater than 1 cm we have a good scanning efficiency at all azimuth angles. Using the range-momentum graph in Review of Particle Properties (RPP), we could

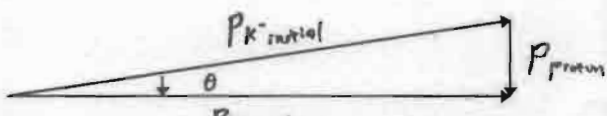


Figure 4: Transfer of momentum from K^- to P_p .

convert the assumption to a momentum of $P_p = 0.143 \text{ GeV}/c$. Then the incident K^- and the scattered K^- have almost the same momentum ($\approx 1.5 \text{ GeV}/c$), and from Fig. 4 we have $P_{K\theta} \approx P_p$. So we obtained $\theta = 0.0935 \text{ rad}$. We know that the differential cross section at small angle has been measured to be approximately $\frac{d\sigma}{dt} = 70 \text{ mbarn}/(GeV/c)^2$ where t is the square of the invariant 4-momentum transfer, and at small angle $t \approx (P\theta)^2$. Therefore we can convert the small angle to the correction for the elastic cross section area (See Fig. 5)

$$t_{\min} \approx (P_K \theta_{\min})^2 = P_p^2 = 20.45 (\text{MeV}/c)^2$$

therefore

$$\Delta\sigma_{el} \approx (\Delta t) \times \left(\frac{d\sigma}{dt} \right) = 0.143 \times 10^{-30} m^2$$

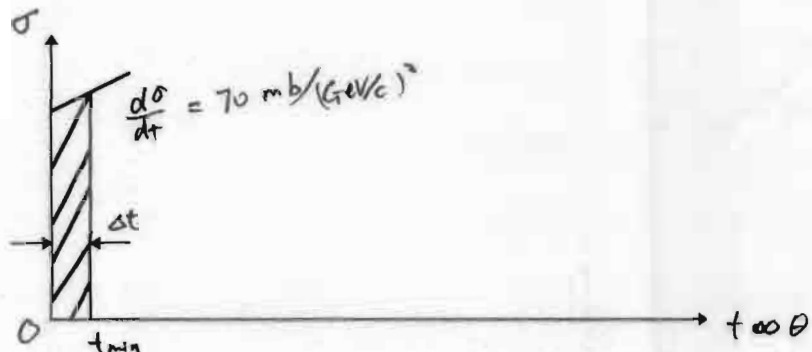


Figure 5: Cross section area versus the square of the invariant 4-momentum transfer.

4) Correction of the systematic error for the number of decays

Since ν is massless, some of the decays such as $K^- \rightarrow \mu^- + \nu_\mu$ will be neglected when these decays occur with nearly zero degree to the incident beam if the momentum change is small. For the decay $K^- \rightarrow \mu^- + \nu_\mu$, the neutrino momentum is (See Appendix 2)

$$P_\nu = \frac{M_{K^-}^2 c^4 - M_\mu^2 c^4}{2(E_{K^-} c + P_{K^-} c^2)} = \underline{37.8 \text{ MeV}/c}$$

Therefore the momentum of muon is

$$P_\mu = \underline{1538 \text{ MeV}/c}$$

which corresponds to the nearly maximum momentum of the muon in the relativistic momentum diagram in Appendix 3. Assume the minimum decay angle at which good scanning efficiency can be realized is $\theta_1 = \theta_2 \approx 0.0953 \text{ radian}$. (See Fig. 6)



Figure 6: Scanning angle.

Since the Kaon is spinless, its decay will be isotropic in the center of mass. The relationship between the lab angle θ and CM angle θ' is

$$\tan \theta = \frac{\sin \theta'}{\gamma_k \left(1 + \frac{\beta_k}{\beta_\mu} \cos \theta' \right)}$$

which for our purposes can be approximated at small angles by $\theta = \theta'/2$. It follows that

$$\theta' = 2\theta = 0.191 \text{ rad} \quad \text{and} \quad \frac{0.191 \text{ rad}}{\cancel{0.191 \text{ rad}}} = 0.0303 \cancel{\text{rad}}$$

Therefore the fraction of kaon decays of 1-prong we miss is simply 6.06% since the angles in Fig. 6 may be below the visible track. We found in Table 3 that the total number of decays is $\Delta N_D = 144$, and from Review of Particle Properties we know that the branching ratio for $K^- \rightarrow \mu_- + \nu_\mu$ mode is 50%. Therefore the corrected value for the number of all decays is

$$\Delta N_\mu = 144 + 144 \times 50\% \times (1 + 6.06\%) = \boxed{149}$$

5) Calculation of K^- life time

Substituting $N_0 = 4900 \pm 200$, $\Delta N_D = 149$, and $\Delta x = 0.2894 \text{ m}$ in to Eqn 4

$$\frac{\Delta N_D}{\Delta x} = \frac{1}{\gamma \beta c \tau} \left(N_0 - \frac{\Delta N_I + \Delta N_D}{2} \right)$$

we obtained

$$\tau = (1.04 \pm 0.05) \times 10^{-8} \text{ sec}$$

The life time of K^- given in Review of Particle Properties is $(1.237 \pm 0.003) \times 10^{-8} \text{ sec}$. Our result does not fall into this range. It is very likely that it is mainly due to the uncertainty of the counting of incident K^- tracks due to the difficulty in determining the parallel incident tracks.

6) Calculation of cross section

Substituting $\Delta N_I = 178$, $\Delta x = 0.2894 \text{ m}$, $N_a = 6.02 \times 10^{23}$, $\rho = 0.06 \text{ gm/cm}^3$, $A = 1.008$, $N_0 = 4900 \pm 200$, and $\Delta N_D = 149$ into Eqn 5

$$\frac{\Delta N_I}{\Delta x} = \frac{N_a \rho \sigma}{A} \left(N_0 - \frac{\Delta N_I + \Delta N_D}{2} \right)$$

we obtained the elastic cross section σ_{el} and total cross area σ_{tot}

$$\sigma_{el} = (0.81 \pm 0.04) \times 10^{-30} \text{ m}^2 \quad \text{and} \quad \sigma_{tot} = (3.47 \pm 0.16) \times 10^{-30} \text{ m}^2$$

Adding the correction obtained at 3) $\Delta \sigma_{el} \approx 0.143 \times 10^{-30} \text{ m}^2$, we obtain

$$\sigma_{el} = (0.82 \pm 0.04) \times 10^{-30} \text{ m}^2 \quad \text{and} \quad \sigma_{tot} = (3.51 \pm 0.16) \times 10^{-30} \text{ m}^2$$

The graph of the cross section versus laboratory K^- beam momentum in the Review of Particle Properties gives the elastic cross section σ_{el} and total cross area σ_{tot}

$$\sigma_{el} = 0.85 \times 10^{-30} \text{ m}^2 \quad \text{and} \quad \sigma_{tot} = 3.30 \times 10^{-30} \text{ m}^2$$

which lie in the ranges we obtained.

7) Calculation of proton's "effective" radius

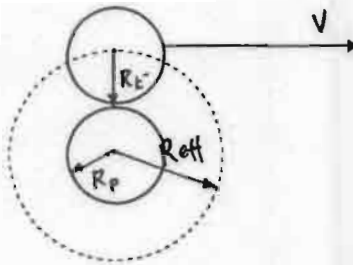


Figure 7: “Geometrical” model in which a K^- sees a proton “effective radius.”

Assume proton and K^- have approximately the same effective radius, then from

$$\sigma_{tot} = \sigma_{geo} = \pi(4R_{eff})^2 = (3.51 \pm 0.16) \times 10^{-30} m^2$$

we have

$$R_{eff} = (5.29 \pm 0.12) \times 10^{-16} m^2 \times 4$$

From the equation

$$r = r_0 A^{1/3} \quad \text{with } r_0 = 1.2 \times 10^{-15} m$$

where A again is the atomic number. Substituting $A = 1.008$ for hydrogen we obtain

$$r = 1.2 \times 10^{-15} m$$

This is twice as large as the effective radius R_{eff} we obtained above. It may be that K^- has a effective radius three times as large as the proton has.

8) Resonance

The total cross-section as a function of beam momentum exhibits “bumps” that are attributed to the formation of a short-lived “resonance” particle. Assuming that the K meson and the proton were to combine to form a single resonant particle at the beam momentum, we would

find the rest mass of the resonance, which is the total combined energy of a incident K^- and a stationary p in the CM frame of these two particles. This CM has a velocity relative to the lab

$$\beta_{CM} = \frac{P_{tot}c}{E_{tot}} = 0.596 \Rightarrow \gamma_{CM} = 1.25$$

where P_{tot} and E_{tot} are the total momentum and energy, respectively, of the K^- and p in the lab frame. Since

$$E_{lab} = \gamma_{CM} E_{CM} = \sqrt{(P_K c)^2 + (M_K c^2)^2} + M_p c^2$$

Therefore we have

$$E_{CM} = 2020 \text{ MeV} \Rightarrow M_{\text{Resonance}} = \frac{2020 \text{ MeV}}{c^2}$$

The quantum numbers of this resonance state are summarized in Table 4

	K^-	p	"resonance"
Electric charge	-1	+1	0
All lepton number	0	0	0
baryon number	0	1	1

Table 4: Quantum numbers of the "resonance."

Since we don't know about the nature of this $K^- + p \rightarrow$ "resonance" interaction, strong or weak, we don't know if flavors are conserved. Even for a strong interaction, spin, isospin, and parity can not be determined because they in general can take on more than one value and depend on the relationship between spin and statistics.

Conclusion

From special relativity we know the measured life time of a particle in a system moving with velocity corresponding to γ with respect to its own rest frame is given by

$$\tau = \gamma \tau_0$$

where τ_0 is the proper life time, which is the life time measured at the particle's rest system.

From our measurement we found τ is very short, and since γ is always larger than or equal to 1, it follows that τ_0 is even smaller. Therefore it is not feasible to measure the K^- lifetime at rest.

This experiment actually provides a way to verify the validity of the special theory of relativity.

We measured the various parameters of K^- and compared them with those of K^+ , with results agreeing within experimental errors. Therefore we can conclude that particles and their corresponding antiparticles have the same mass, the same lifetime, and opposite electric charge. They can be pair-produced from pure energy. This is also a verification of the mass-energy equivalence.

I wrong
In your derivation
you have used the relativity argument already.
So what you measured is the proper lifetime.

Reference

Frauenfelder, Hans and Ernest Henley. "Subatomic Physics". Prentice-Hall, Inc. 1974.

Griffiths, David. "Introduction to Elementary Particle". John Wiley& Sons, Inc. 1987.

Perkins, Donald. "Introduction to High Energy Physics". Addison-Wesley Publishing Company, Inc. Third Ed. 1987.

"Reaction Dynamics for Scanners", Stevenson, M.L.: Physics Notes of Lawrence Berkeley Laboratory: No. 300, Oct. 31, 1986, pp. 1-23.

Review of Particle Properties Rev. Modern Physics 56m 1987.

Tipler, Paul. "Modern Physics". Worth Publishers, Inc. 1969.

Appendices

1) Derivation of the effective number of meson average over the target length

For simplicity let $a \equiv \frac{1}{c\gamma\beta\tau}$ and $b \equiv \frac{N_0\sigma\rho}{A}$ then Eqn. 3 becomes

$$N = N_0 \exp(-ax) \exp(-bx)$$

then the number of K^- average over the target length is

$$N = N_0 \int_0^x \frac{\exp[-(a+b)x]}{\Delta x} dx = \frac{N_0}{-\Delta x(a+b)} \{ \exp[-(a+b)\Delta x] \}$$

Approximate the exponential function to second order of Δx , we have

$$N = \frac{N_0}{-\Delta x(a+b)} \left[1 - 1 - (a+b)\Delta x + \frac{(a+b)^2(\Delta x)^2}{2} \right] = N_0 - \frac{aN_0\Delta x + bN_0\Delta x}{2} \quad (8)$$

Similarly we approximate

$$\begin{aligned} \frac{\Delta N_I}{\Delta x} &= \frac{dN_I}{dx} = aN_0 \quad \text{and} \quad \frac{\Delta N_D}{\Delta x} = \frac{dN_D}{dx} = bN_0 \\ \Rightarrow \Delta N_I &= aN_I \Delta x \quad \text{and} \quad \Rightarrow \Delta N_D = bN_D \Delta x \end{aligned} \quad (9)$$

Substituting Eqn. (9) into Eqn. (8), we obtain

$$N = N_0 - \frac{\Delta N_I + \Delta N_P}{2} \quad (10)$$

2) Calculation of the neutrino and muon momentum in lab frame

Figure 7: Neutrino and muon in Lab frame

Conservation of momentum

$$\vec{P}_{\bar{K}^+} = \vec{P}_{v_\mu} + \vec{P}_\mu \Rightarrow P_{\bar{K}^+} = -P_{v_\mu} + P_\mu \Rightarrow P_\mu = P_{\bar{K}^+} + P_{v_\mu} \quad (11)$$

Conservation of energy

$$E_{K^-} = E_{v_\mu} + E_\mu \Rightarrow E_{K^-} = \sqrt{(P_{v_\mu} c)^2 + (M_\mu c^2)^2} \quad (12)$$

Combining Eqn. (11) and Eqn. (12) and solving for P_{v_n} , we obtain

$$P_{v_\mu} = \frac{M_K^2 c^4 - M_\mu^2 c^4}{2(E_{K^-} c + P_{K^-} c^2)} = 37.77 \text{ Mev} / c^2$$

so

$$P_\mu = 1538 \text{ MeV/c}$$

3) Relativistic vector diagram for $K^- \rightarrow \bar{\mu} + \nu_\mu$ decay

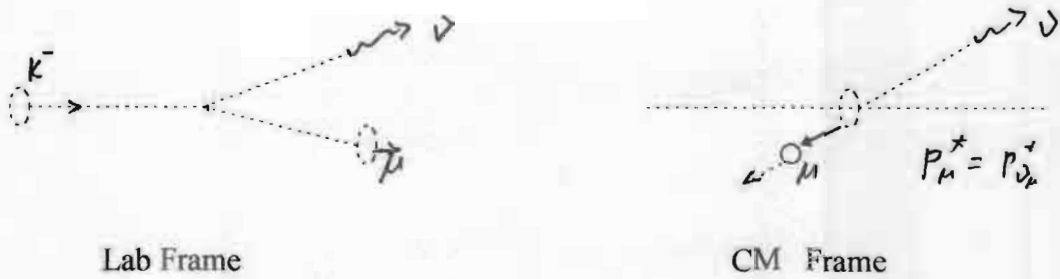


Figure 7: Momenta in lab and CM frames.

From “Reaction Dynamics for Scanners”, we have

$$P_\mu^* = \frac{(M_K c^2 + M_\mu c^2)(M_K c^2 - M_\mu c^2)}{2 M_K c^2} = 236 \text{ MeV/c}$$

$$E_\mu = \frac{(M_K c^2)^2 + (M_\mu c^2)^2}{2 M_K c^2} = 258 \text{ MeV}$$

$$\eta_0 = \frac{P_K}{M_K} = \frac{15 GeV/c}{M_K c^2} = 3.038$$

$$\gamma_0 = \sqrt{\eta_0^2 + 1} = 3.19$$

$$\gamma_0 P^* = 754.4 \text{ MeV/c}$$

$$\eta_0 E_\mu = 783.8 \text{ MeV}$$

Using these values, we can construct momentum vector diagram

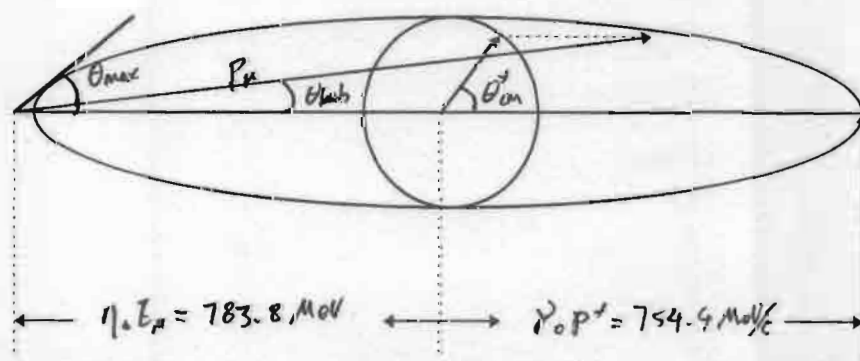


Figure 8: Relativistic Momentum vector diagram for $K^- \rightarrow \bar{\mu} + \nu_\mu$ decay.

$$P_{\mu(\min)} = 783 - 754.4 = 28.6 \text{ MeV} / c$$

$$P_{\mu(\max)} = 783 + 754.4 = 1537 \text{ MeV} / c$$

Therefore Figure 9 shows the diagram when $P_\mu \approx 1537 \text{ MeV} / c$

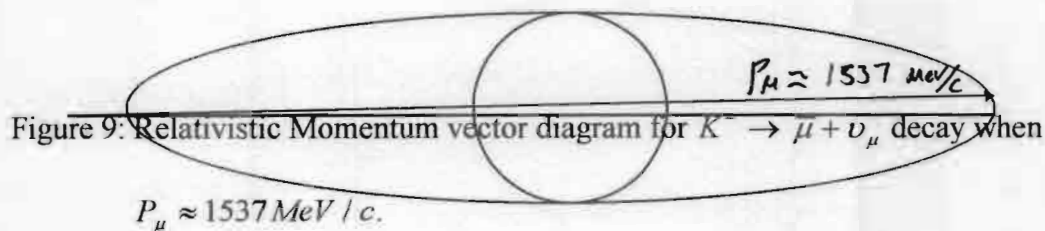


Figure 9: Relativistic Momentum vector diagram for $K^- \rightarrow \bar{\mu} + \nu_\mu$ decay when

$$P_\mu \approx 1537 \text{ MeV} / c.$$

Therefore $\theta_{lab} = \theta_{CM}^* \approx 0^\circ$, and obviously that the decay is hard to detect in this case.

Raw Data

Attached at the end are the raw data taken when scanning the films.

573



$\alpha \rightarrow \beta \rightarrow \gamma \rightarrow \delta$

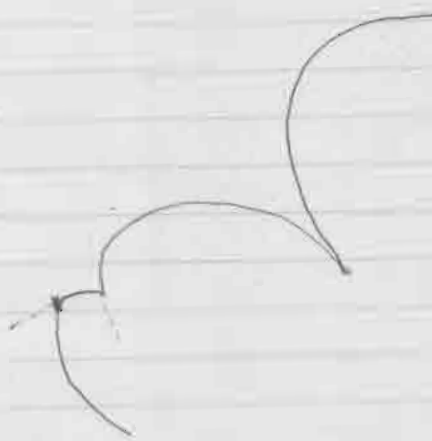
575



623



645

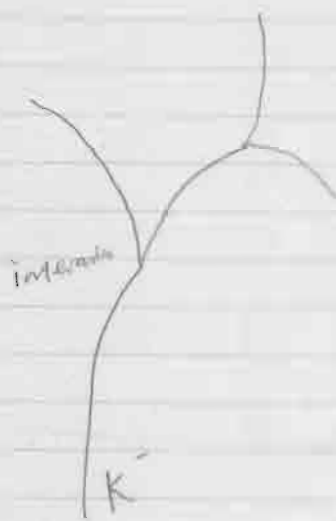


676



67

510



526



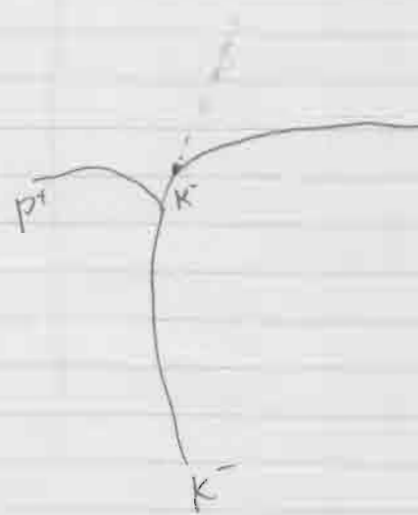
e^-

530

$\bar{\nu}_\mu$



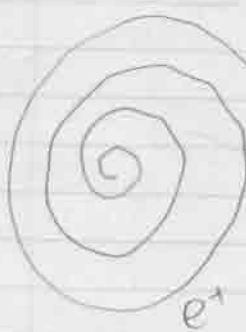
550



510



526

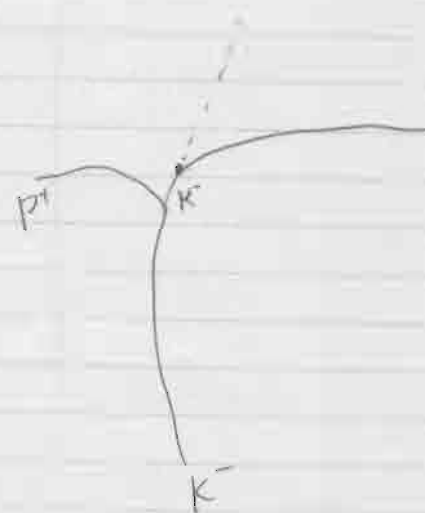


530

$\bar{\nu}_\mu$



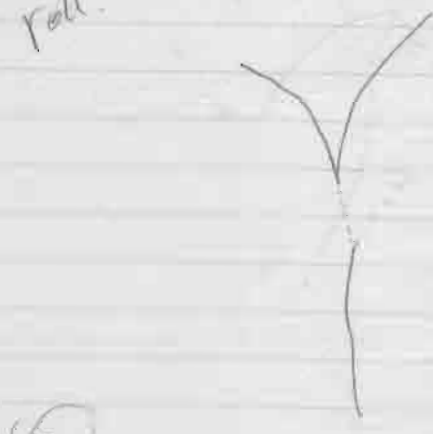
550



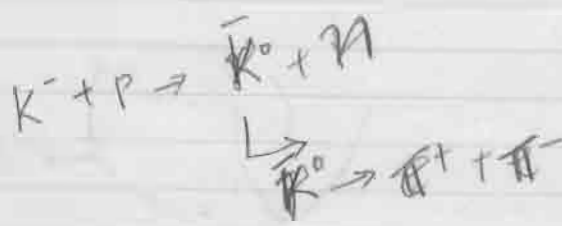
roll # 5450 Frame # 399



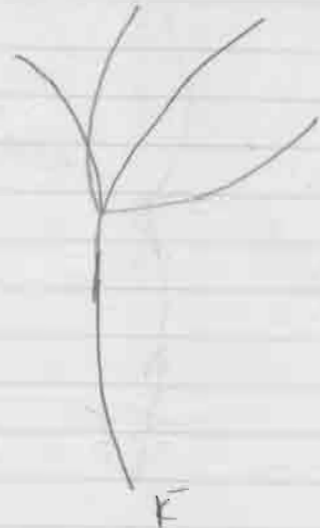
roll # 5450 Frame # 427



(e)



430



Frame # 402



552



559



562.



Frame #438

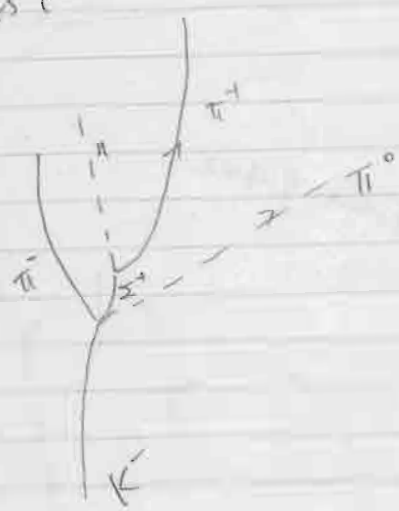


Fwd:

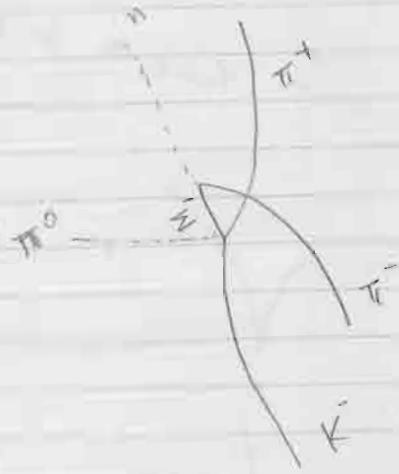
#445



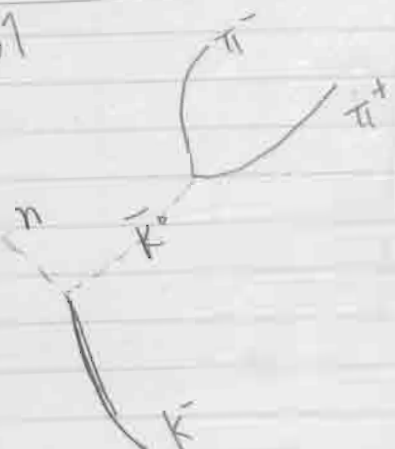
Frame #457



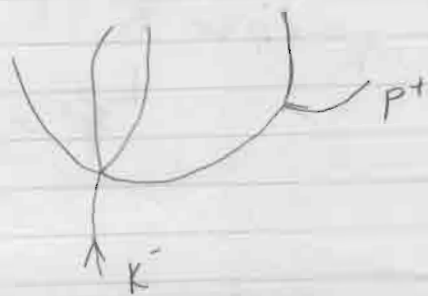
Frame #460



Frame #487



#488



(1)

Roll # 5450

incent tracks	Frame #	Event -	interaction	tau decay	decay	Length	beam
	0394	No	Electric deflection				
	0395	No	the S mag				
	0396						
	0397	No					
	398	No					
	399		2 prong				
13	400	No		the prong			
	401						
	402						
	403	No		2 prong			
	404						
	405						
	406	No					
	407	No					
	408						
	409						
	410		No Prong				
	411						
	412	No					
	413	No					
10	414		2 prongs				
	415		electric				
	416	No					
	417	No					
	418						
	419						
	420	No					
	421	No					
	422	No					
	423						
5	424		2 Prong				

(3)

# Track	Frame #	No Events	Calibration	Innovation	Decay	True Decay	Innovation	Length
11	453	No			1 prong	0.5/100	29.3	
	454				1 prong	0.7/240	3.0	
	455				1 prong	0.7/230	8.2	
	456	No		2 prong		0.3/180°	19.2	
	457			2 prong		0.3/180°	19.2	
	458	No		2 prong		0.3/180°	19.2	
	459			2 prong		0.8/270	0.3	
	460	No			1 prong	0.2/100	23.6	
	461				1 prong	0.2/100	23.6	
	462			2 prong		0.7/180°	17.0	
10	463	No						
	464	No						
	465	No						
	466	No						
	467	No						
	468				1 prong	0.7/230	7.8	
	469	No						
	470				1 prong	0.4/230	12.4	
	471	No						
	472				1 prong	0.7/240	1.9	
10	473			1 prong		0.7/220	10.8	
	474	No						
	475	No						
	476	No						
	477	No						
	478			2 prong		0.8/260°	1.0	
	479	No						
	480			No prong		0.8/220	8.0	
	481			2 prong		0.3/180°	16.1	
	482				1 prong	0.7/230	12.9	
12	483			2 prong	1 prong	0.7/190°	14.6	
	484	No				0.4/260°	9.3	
	485	No						

(2)

Traces	Frame#	No detectors	Events	Collisions	direction	Decay	Tau decay	Location	Length
	415	No			2 prongs			0.4 / 180°	23.2
	426	No						0.5 / 230°	7.2
	427				0 prong + V			0.4 / 180	16.10
	428	No		2 prongs				0.6 / 120°	25.2
	429				2 prongs	1 prong		0.5 / 190°	14.2
	430	No			4 prongs			0.3 / 110°	23.6
	431	No						0.3 / 180°	17.8
	432			2 prong		1 prong		0.3 / 210°	14.5
	433			2 prongs		1 prong		0.3 / 130°	22.3
	434					1 prong		0.4 / 150°	21.4
				2 prong	No prong			0.6 / 140°	22.9
								0.7 / 130°	26.2
8	435	No						0.2 / 260	13.2
	436			2 prong				0.4 / 120	26.0
	437	No		2 prong	2 prong			0.5 / 130	24.0
	438				2 prong	1 prong		0.6 / 140°	23.4
	439		No			1 prong		0.5 / 170°	21.4
	440		No			1 prong			
	441		No			4 prong		0.3 / 190°	17.4
	442					4 prong		0.4 / 250°	10.6
	443					4 prong		0.8 / 260°	3.9
	444				2 prong	1 prong		0.9 / 90°	28.1
11	445		No		2 prong + V			1.0 / 270°	0.4
	446					1 prong		0.9 / 280°	2.1
	447			0 prong		1 prong		0.3 / 280°	10.9
	448			0 prong				0.4 / 220°	12.8
	449	No							
	450			2 prong				0.2 / 230	13.4
	451				1 prong			0.5 / 280	7.2
	452			2 prong + V				0.6 / 230°	5.1

(7)

Frame #	No. ever	# Tracks						
	Entered	Entered	Column	direction	Prong	tan Decoy	location	Length
486	No							
487	No			0 prong + V			0.9/240	4.2
488	No							
489	No					3 prong	8.8/140°	27.1
490	No							
491	No							
492	No							
493	No							
494	No			0 prong			0.3/260	11.2
495	No	5			1 prong		0.4/200	17.5
496	No			0 prong			0.6/250	5.3
497	No						0.7/280°	2.6
498	No							
499	No							
500	No							
501	No							
502	No			0 prong			0.8/240°	4.9
503	No			2 prong + kink			0.4/130°	26.2
504	No							
505	No	6						
506	No							
507	No			1 prong	1 prong		0.7/200	14.7
508	No			2 prong + V	2 prong V		0.9/140°	26.6
509	No			4 prong + L	4 prong		0.7/270°	1.1
510	No			4 prong	1 prong		0.8/240	4.9
511	No			2 prong + C				
512	No			2 prong + kink				
513	No							
514	No							
515	No							
516	No	6						

(5)

#	Tracks	Frame #	No strands	Collision	Interaction	Decay	far decay	location	length
5	517		No		2 prongs + V			0.8 / 240	1.9
	518		No						
	519			2 prong				0.6 / 260	4.6
	520		No	P					
	521						3 prong	0.5 / 240	8.3
	522		No						
	523		No						
11	524				0 prong			0.9 / 110	24.5
	525				4 prong			0.5 / 130	27.2
	526		No						
	527					1 prong		0.9 / 270°	8.4
	528				2 prong			0.8 / 260°	0.5
	529		No						
	530					1 prong		0.6 / 230	9.5
	531		No		2 prong + V			0.5 / 190°	16.3
	532				2 prong + V			0.5 / 230	8.6
	533		No			1 prong		0.7 / 100	20.3
6	534				2 prong			0.4 / 190°	16.1
	535		No						
	536					1 prong		0.2 / 140°	19.4
	537					1 prong		0.8 / 270	0.5
	538				2 prong + V			0.7 / 190	13.5
	539		No						
	540		No						
	541					1 prong		0.6 / 210	11.5
	542		No						
	543				2 prong			0.6 / 230	10.4
					2 prong			0.8 / 250	0.4
12	544					1 prong		0.1 / 190°	19.2
	545					1 prong		0.9 / 240	3.3
	546		No						
	547		No						
	548		No						
	549		No						

(6)

Event	1 Track	Collision 2 prong + ↙	direction	decay	Tau decay	creation	length
550	No event					0.4/180	18.2
551						0.9/240	2.6
552	No						
553	No						
554	No						
555	No	4					
556	No					0.9/140	27.3
557	No					0.8/140	27.5
558	No				1 prong		
559					1 prong + V	0.5/120	25.1
560	No					0.6/150	25.7
561	No						
562						0.8/250	2.2
563	No						
564	No						
565	No	12					
566	No						
567	No					0.4/180	17.1
568	No						
569							
570	No					0.1/80	20.7
571						0.6/140	7.8
572						0.2/230	14.6
573							
574	100					0.4/280	3.3
575						0.5/160	15.8
576						0.6/130	28.1
577	13					0.5/170	17.8
578						0.8/240	5.6
579						0.2/270	12.0
580						0.5/190	14.5
						0.8/250	5.2
						0.5/220	13.7
						0.7/260	3.6

(7)

frames	Frame#	No Event	Collision	Interaction	decay 1 prong	taut decay	location	length
	582	No					0.9/240	1.1
	583	No						
	584	No						
3	585	No						
	586			0 prong				
	587	No						
	588							
	589	No					0.9/230°	0.3
	590	No					0.8/230°	3.3
	591			2 prong			0.2/210°	14.3
	592	No						
	593		2 prong				0.7/240°	6.2
	594							
9	595	No			1 prong		0.8/260°	1.6 cm
	596				1 prong		0.2/180°	16.8
	597						0.5/250	7.7
	598							
	599							
	600							
	601							
	602	No						
	603	No						
	604	No						
10	605			(6)	1-P		0.4/230	9.0
	606				0 prong + V		0.8/240	3.9
	607		2P + kin		2 prong		0.3/190°	16.0
	608	No					0.2/100°	21.6
	609	No					0.5/190°	15.1
	610							
	611	No						
	612	No						
	613	No						
				2 prong			6.5 / 190°	15.1

8

tt Tracks	Frame	No Breaks	Collisions	Decay	Time Decay	Location	Length
9	614	No					
	615	NO					
	616		2P + 2P				
	617			2P			
	618	NO					
	619	NO					
	620	NO					
	621		2P				
	622			CP	1-P		
	623	del		2P + knot			
	624	NO					
9	625	NO					
	626	NO					
	627			2P			
	628	NO					
	629	NO					
	630			2P			
	631		2P				
	632	NO					
	633	NO.					
	634		2P				
8	635	NO					
	636	NO					
	637			4-P + Vtbt			
	638	NO					
	639	NO					
	640	NO					
	641	NO					
	642		2P				
	643	NO					
	644	NO					
	645	NO					
	646						
	647	NO					
11	648			2P			
	649			2P			

(9)

#	Track	Transect	No events	Collars	decoys	decay	Tawdry	Location	Length
	650		No						
	651		No						
	652		No						
	653		No						
	654		No						
7	655		No						
	656		No						
	657		No						
	658		No						
	659		No						
	660					1-P		0.5/120	26.3
	661		No						
	662		No						
	663		No						
	664		No						
6	665					1-P		0.4/180	18.0
	666			2P				0.3/90	23.4
	667		No						
	668			<u>Collars</u> 2P				0.5/100	25.7
	669					1-P		0.8/140	27.0
	670			2P		1-P		0.7/150	24.9
	671			2P				0.8/260	2.4
	672		No					0.9/250	0.6
	673					3P		0.4/150	19.9
	674			2P		1P		0.6/100	29.0
	675		No			1P		0.6/240	6.0
12	676				2P + decay			0.1/90	21.7
	677					1P		0.8/240	6.7
	678					1P		0.3/170	15.0
	679		No		2P			0.7/240	7.6
	680		No		2P			0.6/240	9.0
								0.7/270	4.4

(16)

# Track	Frame #	No event	Collision	duration	decay	time decay	Location	length
6	681			2P			0.5/170	20.8
	682		2P	2P			0.2/60	12.7
	683	.		2P+V			0.6/240	7.3
10	684	No					0.8/220	8.6
	685				1P		0.9/250	2.7
	686			2P			0.3/260	10.7
	687				1P		0.3/110	23.8
	688		2P + Knit		0.02		0.7/240	6.8
	689		2P	2P			0.5/180	16.8
	690			2P+V			0.2/170	18.8
	691				1P+V		0.4/210	13.7
	692	No			1P+V		0.1/170	18.1
	693	No					0.8/250	4.4
	694			2P + Knit			0.6/230	8.7
12	695			2P			Cavier	13.9
	696	No					0.5/230	9.6
	697				1P		0.5/230	10.8
	698			2P-			0.6/230	12.7
	699	No					0.4/250	8.4
	700	No					0.5/130	29.9
	701				1P		0.7/230	9.9
	702						0.7/270	2.5
	703			2P				
	704			2P	1P		0.4/250	10.9
	705	No		2P			0.3/250	9.4
11	706				1P		0.3/120	21.4
	707	No		2P			0.4/120	24.1
					1P		0.4/260	7.7
							0.8/120	28.8
							Cavier	17.1

11

# tracks	Frame#	No Events	Collision	Interaction	decay	tau decay	location	length
	708				1P		0.3/90	24.9
	709				1P		0.9/250	3.7
				2P			0.7/250	7.6
					1P		0.6/130	22.7
				2P			0.5/110	25.9
							0.8/280	0.6
	710							
	711	No					0.6/110	28.5
	712						0.8/270	0.2
	713			2P			0.7/200	12.5
	714	No						
12	715	No						
	716	No					0.7/100	12.5
	717		2P					
	718	No						
	719	No						
	720	No						
	721	No					0.3/270	13.0
	722				1P			
	723	No					0.7/300	4.1
724							6.6/270	4.8
							0.4/320	10.1
14	725			2P				
	726	No						
	727	No						
	728	No						
	729	No						
	730	No						
	731				1P			
	732	No						
	733	No						
	734	No						
	735	No					0.6/240	8.4
	736	No						
	738	No						
	739	1		2P				
	740	No					0.4/320	10.6

(12)

537

610

# Tracks	Frament	Labels	Collision	Orientation	Dong	Tan Decay	Location	length
	742			2-P			0.9/240	1.1
	743				1P		0.5/240	8.5
4	744	No						
	745	No						
	746	No						
	747	No			1P		0.8/270	0.9
	748							
	749	No						
	750	No						
	751	No						
	752	No			1P		0.8/250	3.2
	753				1P		0.7/300	3.0
12	754							
	755	No						
	756	No					0.8/260	0.5
	757	No			1P			
	758	No					0.3/250	10.9
	759				1P		0.2/170	18.9
	760				1P		0.3/270	6.2
	761							
	762							
	763	No						
	764	No						
7	765	No						
	766	No			1P		0.6/260	2.8
	767	No					0.7/230	5.0
	768						0.4/150	22.7
	769				2-P		0.7/230	5.0
	770	No			2-P+bar		0.4/180	17.3
	771							
	772	No						
	773	No					0.7/230	9.1
	774							
10	775	No			4-P			
	776	No					0.8/270	1.1

(13)

#	Frame #	No Event	Collision	Interaction	decay	Final Decay	Location	length
	778	No						
	779	No			2 P		0.2/110	21.6
	780				2 P		0.4/100	26.4
	781	No			2 P		0.2/270	13.0
	782				1 P		0.5/230	10.1
	783	No			0 P		0.7/260	3.6
	784						0.5/290	6.2
6	785	No	2 P				0.1/180	17.5
	786				2 P		0.5/170	19.5
	787	No						
	788	No					0.5/90	26.9
	789		2 P				0.8/140	27.9
	790				1 P			
	791	No			2 P			
	792						0.3/140	22.7
	793	No						
	794	No			2 - P		0.3/190	15.9
15	795							
	796	No			0 - P		0.5/300	8.1
	797						0.6/220	11.6
	798	No			1 P		0.6/170	20.6
	799	No					0.8/280	0.7
	800				1 P		0.2/170	19.5
	801				0 P			
	802	No					0.6/210	11.9
	803		2 P					
	804	No						
14	805	No			2 P		0.6/220	12.7
(14)	806							
	807	No					0.5/190	15.6
	808				1 P		0.5/260	7.4
	809	No			2 P			
	810						0.6/170	19.0

(14)

#	Tracks	Frame #	No Event	Collision	Interaction	Decay	tau Decay	Location	length
13	811		No						
	812		No						
	813		No						
	814		No						
	815			2P					
	816		No						
	817				4P				
	818				2P				
	819				2P				
	820		No		2P+V	1P			
12	821								
	822			2P		1P			
	823								
	824		No						
	825		No						
	826		No						
	827					1P			
	828				2P+V	1P			
	829		No		2P				
	830		No						
10	831		No						
	832				2P+V				
	833				2P				
	834		No						
	835		No						
	836				2P				
	337								
	338		No			1P			
	339								
	340		No						
	341		No			1P			

(15) (15)

Tracks	Name +	No Event	Collision	Interaction	Density	tan(Theta)	Location	length
	842	No						
	843	No						
	844			2P			Center	16.7
7	845						P	
	346				1P	0.8/260	1.6	
	347	No						
	348	No						
	349	100			1P	0.5/240	7.7	
	350	No						
	351	No						
	352	No						
	353			2P		0.6/200	29.5	
10	354	No		2P		0.6/100	29.5	
	355			2P		0.3/100	29.1	
	356	No						
	357	100			1P	0.7/140	25.0	
	358	No						
	359			2P		0.3/150	21.6	
					1P	0.8/270	1.3	
					1P	0.5/300	0.1	
					1P	0.4/300	8.4	
	360				1P	0.9/230	3.3	
					1P	0.7/140	25.8	
					1P	0.6/260	6.0	
	361	No	2P					
	362		2P			0.4/100	27.1	
	363					0.8/250	3.1	
	364					0.6/100	28.8	
11	665			DP		0.6/140	23.1	
11	666				1P	0.3/290	11.0	
	667	No			1P			
	668	No						
	669	No						
	670				1P	0.2/230	14.1	
	671				1P	0.8/250	4.4	
	672				3P	0.8/170	20.5	

(16)	903	No		0 P		0.6/270	3.5
	904	-		2P		0.5/270	6.3
9	905				1P	0.3/180	16.4
# Tracks	875	No Event/ Collision	Interaction	Decay	tau decay	lambda	length
	873		2P + kine			0.9/140	23.5
	874		2P			0.8/270	1.1
14	875			1P		0.7/140	25.2
	876	No				0.7/230	6.7
	877	No					
	878			1P		0.3/240	10.6
	879		4P			0.4/140	24.1
	880			1P		0.2/170	70.7
	881		0P+V			0.8/280	7.8
	882			1P		0.2/180	17.4
	883	No					
	884		0P+V	0P		0.4/260	8.5
	885		2P+<			0.7/220	9.9
	886		2P			0.8/176	21.2
10	885			1P		0.1/120	19.4
	886	No				0.5/170	19.4
	887		2P			0.5/170	19.2
	888				1P	0.7/290	1.4
	889	No					
	890				1P	0.9/250	0.3
	891	No		2P		0.4/60	27.6
	892					0.2	12.4
	893				1P	0.3/270	12.4
	894				1P	0.8/60	0.8
11	895				1P	0.7/260	3.5
	896		2P			0.8/270	1.4
	897	No		2P		0.2/170	19.7
	898					0.6/160	21.2
	899	No					
	900				1P	0.4/180	17.6
	901		2P				
	902				1P	0.8/270	1.3
					1P	0.2/90	23.5
					1P	0.9/210	0.4
					1P	0.3/180	17.3